DOT/FAA/CT-89/20

**FAA Technical Center**
Atlantic City International Airport
N.J. 08405

# Development of an Advanced Fan Blade Containment System

Alan D. Lane
Advanced Structures Technology, Inc.
Phoenix, Arizona

FEDERAL AVIATION ADMINISTRATION
JUL 13 1999
TECHNICAL CENTER LIBRARY
ATLANTIC CITY INT'L AIRPORT, NJ 08405

August 1989

Final Report

**This document is available to the U.S. public through the National Technical Information Service, Springfield, Virginia 22161.**

U.S. Department of Transportation
**Federal Aviation Administration**

FAA WJH Technical Center
Tech Center Library
Atlantic City, NJ 08405

**DOT/FAA**
**CT-89/20**

AVAILABLE IN
ELECTRONIC FORMAT

NOTICE

This document is disseminated under the sponsorship of the U. S. Department of Transportation in the interest of information exchange. The United States Government assumes no liability for the contents or use thereof.

The United States Government does not endorse products or manufacturers. Trade or manufacturers' names appear herein solely because they are considered essential to the objective of this report.

**Technical Report Documentation Page**

| 1. Report No. | 2. Government Accession No. | 3. Recipient's Catalog No. |
|---|---|---|
| DOT/FAA/CT-89/20 | | August 1989 |

| 4. Title and Subtitle | 5. Report Date |
|---|---|
| DEVELOPMENT OF AN ADVANCED FAN BLADE CONTAINMENT SYSTEM | 6. Performing Organization Code |
| 7. Author(s) Alan D. Lane | 8. Performing Organization Report No. AST89004 |
| 9. Performing Organization Name and Address<br>Advanced Structures Technology, Inc.<br>2849 South 44th Street<br>Phoenix, Arizona 85040 | 10. Work Unit No. (TRAIS)<br>11. Contract or Grant No. DTRS-57-88-c-00117 |
| 12. Sponsoring Agency Name and Address<br>Department of Transportation<br>Federal Aviation Administration<br>Technical Center<br>Atlantic City International Airport, NJ 08405 | 13. Type of Report and Period Covered<br>Final Report<br>10/11/88 to 4/7/89<br>14. Sponsoring Agency Code ACD-210 |

15. Supplementary Notes

Project Manager: Bruce C. Fenton - FAA Technical Center

16. Abstract


The objective of this fan blade containment study was to investigate potential weight savings using a ceramic-based blade containment system. Technology developed to provide light-weight armor for aircraft and aircrew members has shown that systems using ceramics ($Al_2O_3$, SiC, and $B_4C$) are more weight efficient than metals (steel, titanium, and aluminum), or polymer fibers (fiberglass and Kevlar™).

The study consists of three primary sub-tasks:

1. Design a ceramic-based fan blade containment system to achieve the maximum possible weight effectiveness.

2. Compare the ceramic containment system with current metal and Kevlar systems to quantify the potential weight improvement and corresponding cost impact.

3. Develop a test plan, including the design of test fixtures and test articles to allow verification of improved weight effectiviness of ceramic-based systems.


| 17. Key Words | 18. Distribution Statement |
|---|---|
| Aircraft Hazards<br>Aircraft Safety<br>Fan Blade Containment<br>Turbine Engine Containment<br>Ceramic Material Technology | Document is available to the public through the National Technical Information Service, Springfield, Virginia 22161 |

| 19. Security Classif. (of this report) | 20. Security Classif. (of this page) | 21. No. of Pages | 22. Price |
|---|---|---|---|
| Unclassified | Unclassified | 34 | |

Form DOT F 1700.7 (8-72) Reproduction of completed page authorized

TABLE OF CONTENTS


| Section | Page |
|---|---|
| Executive Summary | vii |
| 1. Introduction | 1 |
| 1.1 Mechanics of Containment | 2 |
| 2. Technical Discussion | 5 |
| 2.1 Literature Search | 5 |
| 2.2 Definition of Containment System Requirements | 5 |
| 2.3 Metallic Containment Ring Design | 11 |
| 2.4 Kevlar Containment System Design | 12 |
| 2.5 Ceramic-Based Containment System Design | 13 |
| 2.5.1 Direct Application of Armor Test Data to Containment Ring Design | 15 |
| 2.5.2 Correlation of Armor and Actual Containment Design Information to Calculate $B_4C$/Spectra Thickness Requirements | 17 |
| 3. Conclusions | 22 |
| 4. References | 22 |
| 5. Bibliography | 24 |
| Appendix A - BASIC Program for Calculation of Blade Energy | |

## LIST OF ILLUSTRATIONS


| Figure | | Page |
|---|---|---|
| 1 | Schematic of Containment Ring Failure Due to Large Plastic Deformation Following Disk Burst | 3 |
| 2 | Example of Containment Ring Penetration by a Fan Blade | 4 |
| 3 | Relationship of Engine Thrust to Fan Tip Diameter | 7 |
| 4 | Predicted Kinetic Energies and Blade Geometry (without lean, twist, or camber) for Representative Turbofan Engines | 9 |
| 5 | Predicted Fan Blade Kinetic Energies for Several Turbofan Engines | 10 |
| 6 | Kevlar Containment Ring Thickness Versus Fan Blade Kinetic Energy | 14 |
| 7 | Titanium Containment Ring Thickness Based on THOR Equations | 16 |
| 8 | Ratio of Kevlar to $B_4C$/Spectra Areal Density versus Fan Blade Kinetic Energy | 18 |
| 9 | Ratio of Kevlar to $B_4C$/Spectra Thickness Versus Fan Blade Kinetic Energy | 19 |
| 10 | Kevlar and $B_4C$/Spectra Containment Ring Areal Density Versus Blade Kinetic Energy | 20 |
| 11 | Kevlar and $B_4C$/Spectra Containment Ring Thickness Versus Blade Kinetic Energy | 21 |

## LIST OF TABLES


| Table | | Page |
|---|---|---|
| 1 | Ceramic Properties | 5 |
| 2 | Representative Data for Current Turbofan Engines | 8 |
| 3 | Comparison of Predicted and Published Blade Energies | 11 |

## EXECUTIVE SUMMARY

This report presents the results of a study of turbine engine fan blade containment systems performed for Phase I of a DOT/FAA sponsored Small Business Innovation Research contract. The 180-day program was initiated on October 11, 1988, and was conducted in accordance with Department of Transportation Contract No. DTRS-57-88-C-00117.

The objective of the study was to investigate potential weight savings using a ceramic-based blade containment system. Technology developed to provide light-weight armor for aircraft and aircrew members has shown that systems using ceramics ($Al_2O_3$, SiC, and $B_4C$) are more weight efficient than metals (steel, titanium, and aluminum), or polymer fibers (fiberglass and Kevlar™). It is expected that this technology can provide similar weight savings for turbine engine containment systems.

Phase I consisted of three primary sub-tasks:

a. Design a ceramic-based fan blade containment system to achieve the maximum possible weight effectiveness. This sub-task included a literature search to ensure that current state-of-the-art technology, for both blade containment and armor design, would be used.

b. Compare the ceramic containment system with current metal and Kevlar systems to quantify the potential weight improvement and corresponding cost impact.

c. Develop a test plan, including the design of test fixtures and test articles to allow verification of improved weight effectiveness of ceramic-based containment systems during Phase II. The Phase II test plan is the subject of a SBIR Phase II proposal and not included herein.

Conclusions reached during the program were:

a. Armor test data show that $B_4C$/Spectra is more weight effective than Kevlar for defeating projectile penetration.

b. The ratio of $B_4C$/Spectra weight effectiveness to that of Kevlar is larger for higher kinetic energy projectiles.

c. The weight effectiveness of $B_4C$/Spectra versus Kevlar containment is significant for engines of 20000 lb. or greater thrust.

## 1. INTRODUCTION

Although highly reliable, modern turbine engines have the potential for seriously damaging the aircraft on which they are mounted. Fan, compressor, and turbine rotors possess large rotational kinetic energies that can cause damage or injury to aircraft structure, systems, and occupants if fragments created by a rotor failure are not contained within the engine nacelle structure.

The potential for mishap is recognized in the Federal Aviation Regulations, Part 33 (Airworthiness Standards, Aircraft Engines), Section 33.94, which requires that an engine's ability to contain a failure of the critical fan and turbine blades be substantiated by test.

Containment is generally accomplished by placing a metal, or composite, ring around critical components so that rotor fragments can not penetrate the ring and escape the nacelle. The containment ring is placed as near the rotor as is practical to reduce the ring diameter, length, and weight to the lowest possible value.

To minimize weight, materials with the highest available specific energy absorption capacity are used. These are materials able to absorb large amounts of kinetic energy for a given weight of containment material. One such material, Kevlar fiber, has gained wide use for fan blade containment on engines developed within the last decade. However, Kevlar and other polymer fibers do not have the high temperature tolerance required for use in the hot section of the engine (high-pressure compressor and turbine sections).

The need for light-weight systems to prevent projectile penetration is not confined to turbine engine containment. The same requirement exists for armor to protect military aircraft and their crews. The technology for aircraft/aircrew armor has progressed along lines similar to fan containment rings, starting with high strength steels, followed by alternate metals (aluminum, titanium), and polymer fibers (fiberglass, Kevlar). The latest state-of-the-art materials used for armor are structural ceramics (alumina, boron carbide). These materials used in combination with polymer fibers have proven to be more weight efficient than previous armor materials.

The objective of this program was to investigate the application of the ceramic armor system concept to fan blade containment structures. It is expected that the weight improvement gained by the use of ceramic-based armor systems can be transferred to blade containment systems. Since ceramics retain their strength to temperatures of 2400°F or greater, they offer the potential for use in the hot section

of turbine engines. Thus ceramic systems offer the potential of weight efficiency superior to Kevlar, plus high temperature properties that would allow their use in the hot turbine section of the engine.

## 1.1 Mechanics of Containment

There are two distinct modes of containment failure to be considered. One mode is large magnitude plastic elongation, and subsequent tensile failure of the containment ring under forces induced by deceleration of large, high energy fragments created by the burst of an entire disk. This type of failure is illustrated schematically in figure 1.

To contain a disk burst, rings must be highly ductile to allow large plastic elongations prior to tensile failure. This permits the kinetic energy of the disk fragments to be converted to strain energy though large plastic deformation of the containment ring. At the same time, the ring must have high compressive strength and fracture toughness to prevent disk fragments from piercing the ring and escaping. A typical material used for containment in the hot turbine section of the engine is INCONEL 625 which provides values of 30 percent tensile elongation combined with relatively good tensile strength (120,000 psi).

The second containment ring failure mode is penetration of the containment structure by small fragments, typically produced by blade or dovetail failures. In this mode, the containment ring remains intact, but with a hole caused by penetration of the blade (or other) fragment. An example of this is shown in figure 2 which shows the outer surface of a containment ring following penetration by a fan blade.

It is the second failure mode (penetration) that ceramic systems are best suited for preventing. Ceramics are extremely hard materials with high compressive strength that can cause local deformation and fracture of the blade on impact, thereby reducing the effective penetration weight of the blade. The polymer backing material used with the ceramic serves to prevent spalling of the ceramic after blade impact, and provides the capacity for plastic, tensile, elongation to absorb the kinetic energy of the blade. The mechanical properties of ceramic materials commonly used in military armor systems are shown in table 1.

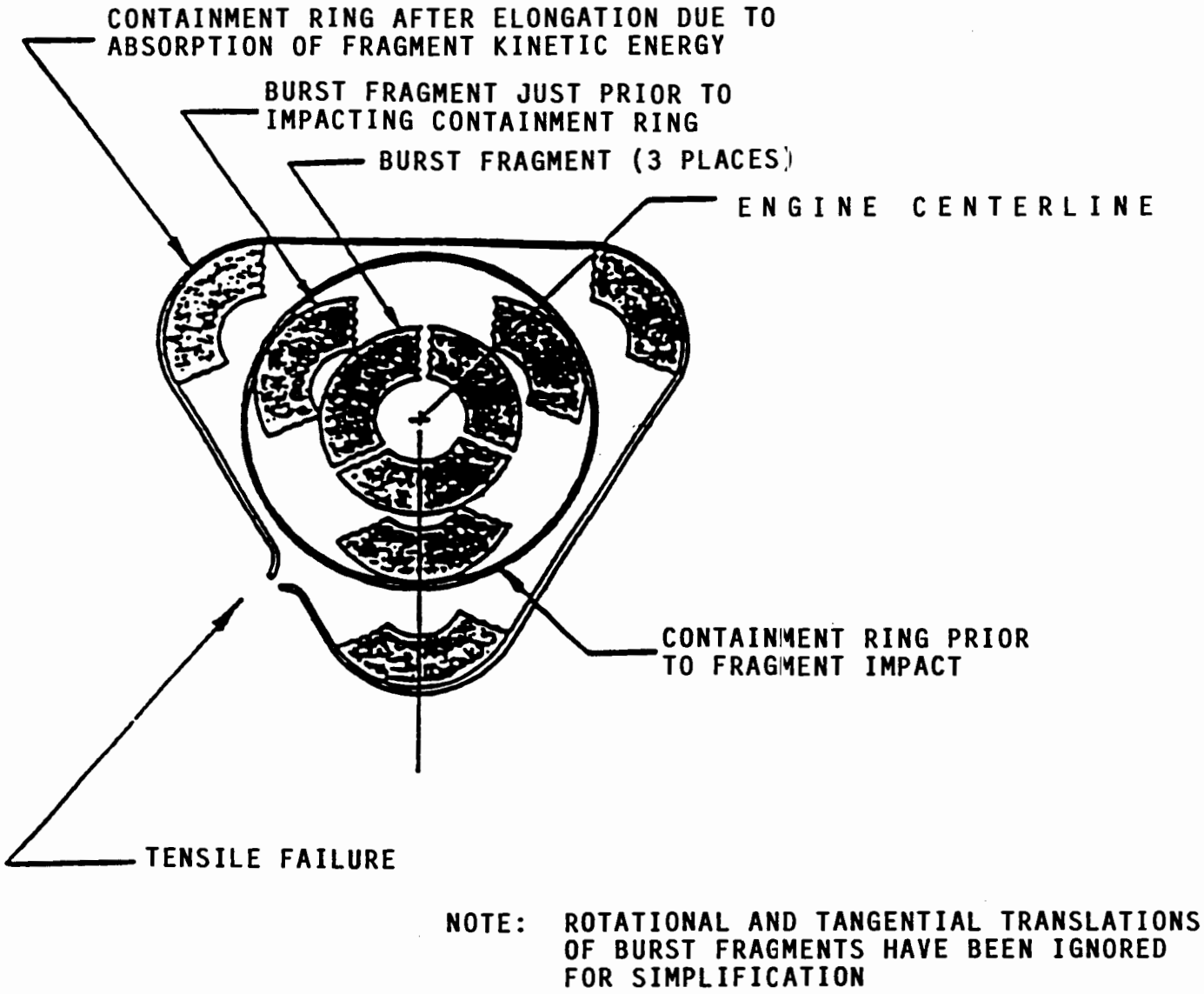


NOTE: ROTATIONAL AND TANGENTIAL TRANSLATIONS OF BURST FRAGMENTS HAVE BEEN IGNORED FOR SIMPLIFICATION

FIGURE 1. SCHEMATIC OF CONTAINMENT RING FAILURE DUE TO LARGE PLASTIC DEFORMATION FOLLOWING DISK BURST

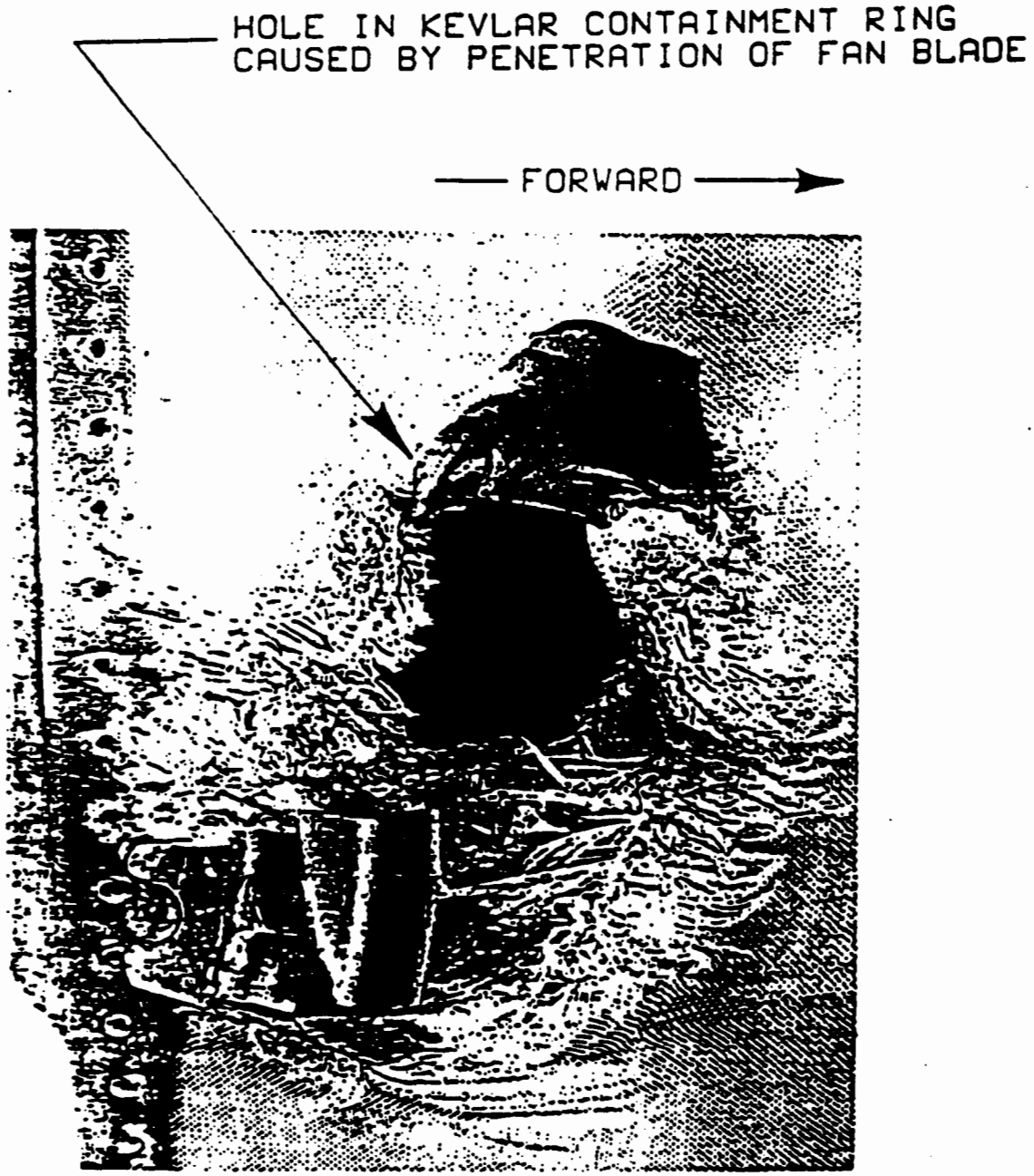


NASA/GE
REFERENCE 4

FIGURE 2. EXAMPLE OF CONTAINMENT RING PENETRATION BY A FAN BLADE

TABLE 1
CERAMIC PROPERTIES

| Ceramic | Specific Gravity | Compressive Strength (psi) | Modulus of Elasticity (psi) | Hardness (Knoop 1000 G Load) |
|---|---|---|---|---|
| $B_4C$ | 2.52 | 400,000 | $68 \times 10^6$ | 29 |
| SiC | 3.14 | 580,000 | $60 \times 10^6$ | 25 |
| $Al_2O_3$ | 3.41 | 290,000 | $32 \times 10^6$ | 10 |

Containment rings add significant weight to an engine, with a resulting addition of many pounds to overall airframe weight. To achieve lower weight, Kevlar has been used on many recent fan containment systems. Some of the polymer fibers, of which Kevlar is one example, provide better penetration and elongation properties than a comparable weight metal system. However their use is restricted to the relatively cool fan section of the engine because they do not have the temperature resistance necessary for the high pressure compressor and turbine sections of the engine.

## 2. TECHNICAL DISCUSSION

### 2.1 Literature Search

A data search for technical papers pertaining to turbine engine containment, use of ceramics in turbine engines, and lightweight armor systems, was performed by Advanced Structures Technology, Inc. (AST), Simula, Inc., and the Fee-Based Information and Research Service Team at Arizona State University, Tempe, Arizona.

The data in the technical papers were used to determine design equations currently used by turbine engine designers to size containment rings (references 1, 2, 3, 4). The design equations obtained from the technical papers were used to calculate the required thicknesses of Kevlar containment rings for engine sizes ranging from 1,300 to 54,000 lb. thrust. The papers contained information regarding kinetic energies of some current production fan blades. (Sec. 2.4).

### 2.2 Definition of Containment System Requirements

This section describes the procedure used to develop a representative threat for which Kevlar and ceramic-based containment systems were designed. A threat (failed blade)

model was developed that allowed the relative effectiveness of Kevlar and ceramic-based containment systems to be quantified for a wide range of engine thrust levels. The geometry (thickness and length) of a fan blade containment structure is dictated by the following parameters:

a. Kinetic energy of the blade.

b. Geometry of the blade (thickness, chord length, span, twist, etc.).

c. Mechanical properties of the containment material (dynamic shear strength, ductility, tensile strength).

In order to define items a and b, a mathematical fan blade model was developed to calculate fan blade kinetic energy and geometry as a function of engine thrust. The model was based on several observed relationships that are representative of design practice for recent turbofan engines. These parametric relationships are:

a. Fan blade tip speed is relatively constant regardless of engine size (approximately 1485 ± 100 ft/sec.).

b. Fan solidity (chord length/blade spacing) is approximately 2.75 at the hub and 1.15 at the tip.

c. Hub diameter/tip diameter ratio is between 0.33 and 0.38.

d. Blade thickness is approximately 0.0275 times chord length at the tip, and 0.065 times chord length at the hub.

The published tip diameter, blade count, and thrust for several modern turbofan engines were obtained from reference 5. The engine model numbers, tip diameters, blade count, and thrust are presented in table 2.

A regression analysis of the data in table 2 was used to obtain a relationship between thrust and fan tip diameter. The resulting relationship is shown in figure 3.

The tip diameters and number of blades shown in table 2 were used to calculate corresponding tip and hub chord lengths, hub diameter, blade thicknesses at tip and hub, weight, and center of gravity location. This information coupled with the approximate tip speed allows the blade rotational kinetic energy to be calculated. A BASIC program written to perform these calculations is presented in Appendix A.

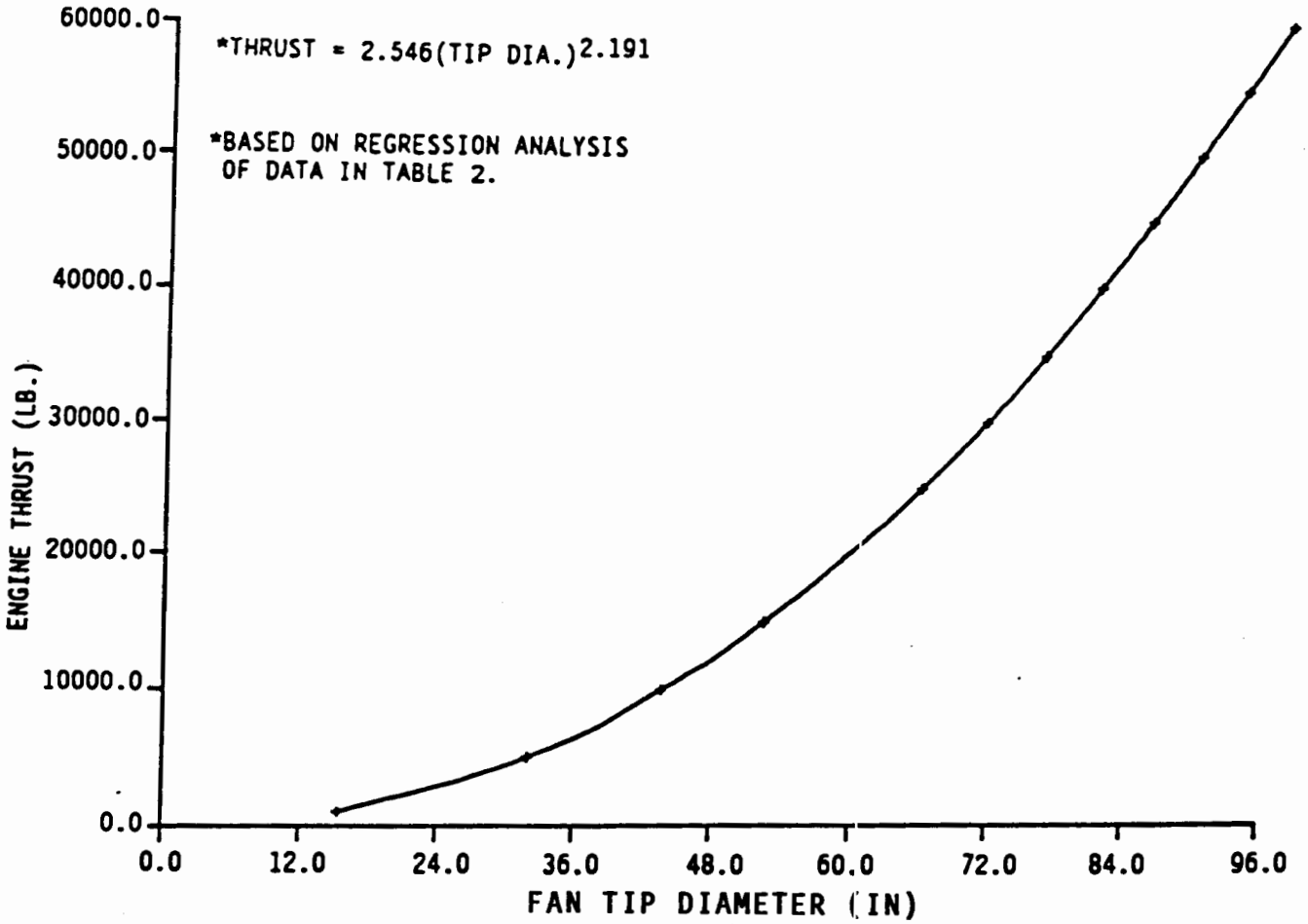


FIGURE 3. RELATIONSHIP OF ENGINE THRUST TO FAN TIP DIAMETER

TABLE 2
REPRESENTATIVE DATA FOR CURRENT TURBOFAN ENGINES

| Model Number | Thrust (lbf) | Diameter (in.) | Blade Count |
|---|---|---|---|
| F109 | 1330 | 18.25 | 30 |
| TFE731-2 | 4500 | 28.2 | 30 |
| CFM56-2 | 24000 | 70.5 | 44 |
| PW2037 | 38250 | 78.5 | 36 |
| JT9D-7 | 45600 | 93.4 | 46 |
| CF6-6D | 45750 | 86.4 | 38 |
| RB211-524D4 | 53000 | 86.3 | 33 |
| JT9D-7R4G | 54750 | 94.9 | 40 |

The methodology described above was used to calculate the fan blade kinetic energies for several engines. Predicted kinetic energies, and geometries of the fan blades (without lean, twist, or camber) are shown in figure 4. A comparison of the predicted energies with published values for two actual blades is presented in table 3, and a plot of predicted blade energy versus thrust, for several common engines, is presented in figure 5. The model predictions are expected to be accurate to within 10 percent.

The blade geometries and kinetic energies shown in figure 4 were used as a standard threat for which Kevlar and ceramic-based containment systems were designed and evaluated. The use of the standardized blade model allowed all containment systems to be compared against a common threat, covering the entire thrust range of current in-service commercial turbofan engines.

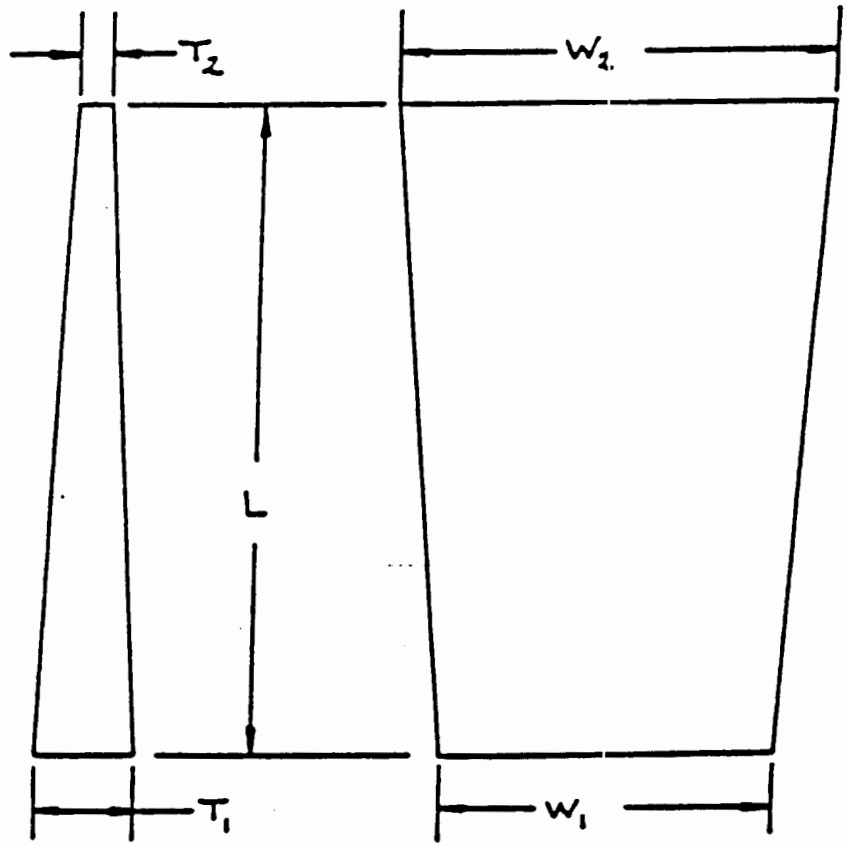


| MODEL NUMBER | NUMBER OF BLADES | WEIGHT (LB) | K.E. (IN-LB) | L (IN) | $W_1$ (IN) | $W_2$ (IN) | $T_1$ (IN) | $T_2$ (IN) | THRUST (LB) |
|---|---|---|---|---|---|---|---|---|---|
| JT9D-7 | 46 | 9.39 | $(1.6)(10^6)$ | 31.30 | 5.79 | 7.34 | .376 | .202 | 45600 |
| CFM56-2 | 44 | 4.41 | $(7.5)(10^5)$ | 23.62 | 4.57 | 5.79 | .297 | .159 | 24000 |
| TFE 731-5 | 30 | .47 | $(1.03)(10^5)$ | 9.45 | 2.68 | 3.40 | .174 | .093 | 4500 |
| F109 | 30 | .25 | $(2.8)(10^4)$ | 6.11 | 1.73 | 2.20 | .113 | .060 | 1330 |
| CF6-6D | 38 | 10.89 | $(1.85)(10^6)$ | 28.94 | 6.48 | 8.21 | .421 | .226 | 45750 |
| TEST ARTICLE | 40 | 3.29 | $(5.6)(10^5)$ | 20.10 | 4.28 | 5.42 | .278 | .149 | 20000 |

FIGURE 4. PREDICTED KINETIC ENERGIES AND BLADE GEOMETRY (WITHOUT LEAN, TWIST, OR CAMBER) FOR REPRESENTATIVE TURBOFAN ENGINES

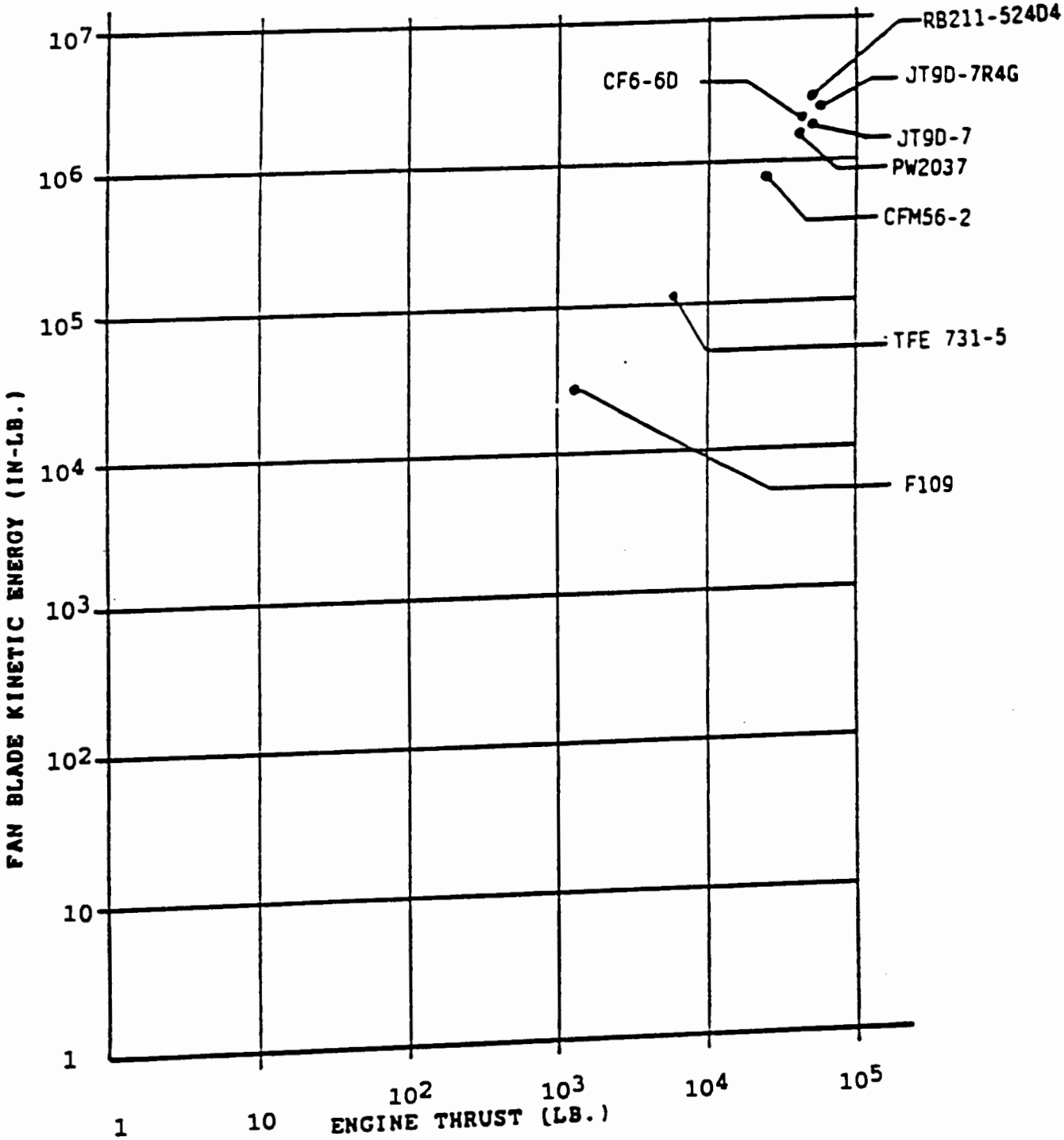


FIGURE 5. PREDICTED FAN BLADE KINETIC ENERGIES FOR SEVERAL TURBOFAN ENGINES

TABLE 3
COMPARISON OF PREDICTED AND PUBLISHED BLADE ENERGIES

| ENGINE MODEL NO. | AST, INC. BLADE ENERGY MODEL (IN-LB.) | PUBLISHED FAN BLADE ENERGY (IN-LB.) | ENGINE THRUST (LB.) |
|---|---|---|---|
| JT9D-7 | 1,600,000 | 1,590,000* | 45,600 |
| CF6-6 | 1,856,000 | 1,872,000** | 45,750** |

* reference 2
** reference 3

## 2.3 Metallic Containment Ring Design

An objective of Phase I was to compare the weight effectiveness of ceramic-based containment systems to existing metal and Kevlar containment systems. Metal fan containment rings have been generally fabricated from stainless steel, aluminum, or titanium. As discussed below, it was possible to obtain only enough data from open publications to allow the use of one major engine manufacturer's metallic containment ring design equation. This was not considered sufficient to ensure that a design representative of the entire turbine engine industry could be developed.

Since Kevlar has been shown to be more weight effective than the metals (references 3 and 4), it is the material which ceramic-based containment systems must surpass. Thus the shortage of public design data for metallic containment rings did not adversely impact the principal objective of demonstrating reduced containment system weight using ceramic-based designs.

As part of the Phase I literature search, information was found concerning design of metallic containment structures. A summation of published design equations used for sizing metal containment structures is presented below.

United Technologies:

$t = K_1 \cdot [(B \cdot KE) \div (Uds \cdot P)]^{1/2}$ (reference 2)

General Electric Corp.:

$t = K_2 \cdot (KE)^{1/2}$ (reference 4)

Snecma:

$t = \sin(\alpha)\cdot[(KE)\div(Uds\cdot P)]^{1/2}$ (reference 1)

Where:

$t$ = containment ring thickness.
$KE$ = blade translational kinetic energy.
$K_1$, $K_2$, = empirically developed constants.
$B$ = blade buckling factor.
$P$ = perimeter of shear plug.

** $Uds$ = dynamic shear strength.

$\alpha$ = blade impact angle.

** For Titanium Uds = 145,000 psi (reference 7)

A review of the methodology reported above shows that all analytical sizing techniques, while similar, contain empirically derived constants ($K_1$, $K_2$, B, Uds). Except for the values of Uds quoted in reference 7, these empirical constants are proprietary to the individual manufacturer and not available to allow comparative design of metallic containment systems.

## 2.4 Kevlar Containment System Design

The design of Kevlar containment rings is especially important to the evaluation of ceramic-based systems, because Kevlar rings are the most weight efficient containment structures in use on current engines. For this reason the comparison of ceramic-based systems to Kevlar will determine whether ceramics can provide an improvement in containment system weight efficiency. This section describes the technology currently available for the design of Kevlar systems.

Considerable research has been performed regarding the design of Kevlar containment systems (references 3, 4, 6.f to 6.1, 7). Detailed design information based on testing performed by General Electric under contract to NASA is available (references 3 and 4). The basic equation that is available from the NASA/GE research is based on kinetic energy of the blade fragment, and contains an empirical constant obtained from actual spin pit containment testing. The design equation is:

$t = K \cdot (KE)^{1/2}$

t = minimum Kevlar thickness for containment (inch).
KE = blade kinetic energy (ft-lb)
K = empirical constant = 0.00141 (reference 3, rotor tests)
0.00264 (reference 4, rotor tests)
0.00341 (reference 4, gas gun tests)

The values of K obtained during the testing reported in reference 4 (NASA/GE) were obtained from subscale gas gun and rotor tests. The values given in reference 3 (NASA/GE) were obtained from full scale spin pit testing using a TF34 fan. The optimized full scale spin pit testing is most representative of actual engine operation and should be the most accurate design tool.

The relationship of thrust and Kevlar containment ring thickness using all three values of K listed above are shown in figure 6 . Curve No. 1 in figure 6 is based on data obtained during spin pit testing (reference 3) and should be the most accurate of the three with regard to required Kevlar containment ring thickness. Phase I results and Phase II planning are based on Kevlar rings sized using the relationship represented by curve 1 (K = 0.00141) in figure 6.

## 2.5 Ceramic-Based Containment System Design

The steps followed in selecting materials and sizing a ceramic-based containment ring are briefly outlined below. Detailed discussions of each item is presented in Sections 2.5.1 through 2.5.3.

Step 1. Armor test panel data were used to directly predict the required thickness for a titanium containment system as a basis for checking to see if this would be a viable design technique.

Step 2. The predicted containment ring thicknesses obtained from step 1 above were compared with actual in-service production hardware. The correlation between predicted and actual in-service designs was very poor.

Step 3. As a result of step 2, it was concluded that armor test panel data, while suitable as a screening test to obtain the relative effectiveness of candidate systems, cannot be used to directly calculate containment ring thickness requirements. Since spin pit containment tests with Kevlar rings and fan blades (see Section 2.4) more closely simulates an actual engine environment than do gas gun or ballistic armor test panel tests, the Kevlar ring was

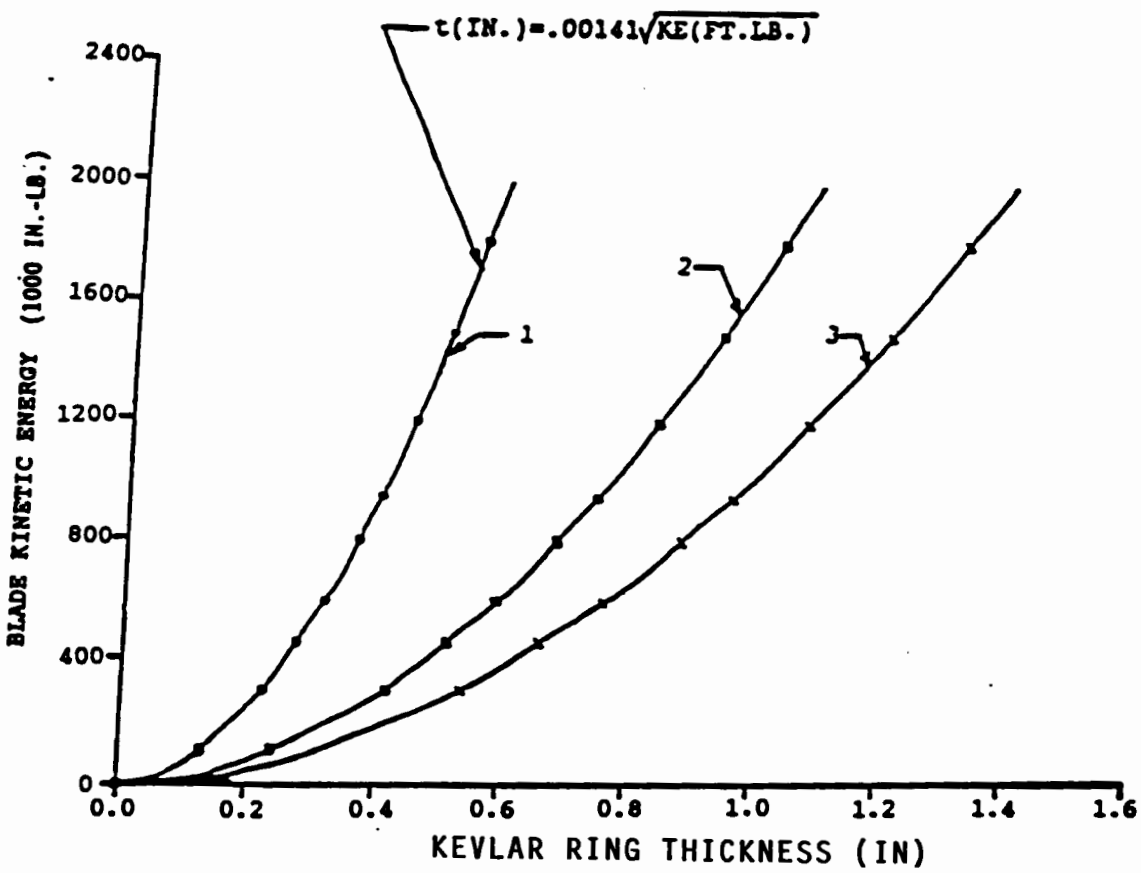


1 NASA/GE FINAL, ROTOR SPIN PIT TEST DATA

2 NASA/GE INITIAL SPIN PIT ROTOR DATA

3 NASA/GE GAS GUN TEST DATA

FIGURE 6. KEVLAR CONTAINMENT RING THICKNESS VERSUS FAN BLADE KINETIC ENERGY

designed using the data in Section 2.4, rather than extrapolating from armor test panel data.

Step 4. The final ceramic-based containment system was designed by using containment test data (See Section 2.4) to determine the required Kevlar ring thickness for a range of engine thrusts. Armor test panel test data were used to compare alumina and boron carbide armor systems with Kevlar in the areal density range obtained for the Kevlar from the spin pit containment test data.

### 2.5.1 Direct Application of Armor Test Data to Containment Ring Design

The Project THOR equations (reference 9) are a set of empirical equations derived to fit armor test data. Simula, Inc., proprietary data, presented as supporting documentation from reference 8, were used to provide the empirical constants for the following ceramic-based armor systems:

1. $B_4C$/SPECTRA
2. $B_4C$/KEVLAR
3. SIC/SPECTRA
4. SIC/KEVLAR
5. $Al_2O_3$/SPECTRA
6. $Al_2O_3$/KEVLAR

Reference 8 summarizes the capability of the materials, based on the results of ballistic testing with projectiles ranging from 22 caliber to 20 millimeters and fired at velocities from 600 to 5750 ft/sec. The tests typically consist of firing the projectile at 12-inch (or less) square test panels that are rigidly mounted to a heavy fixture.

The data indicate that $B_4C$/Spectra is the most weight effective of the ceramic-based systems listed above. Therefore $B_4C$/Spectra was selected as the system to be used for design of a ceramic-based containment system.

To check the validity of the THOR equations for directly predicting containment ring thickness, sample calculations were made using the properties of titanium. The thickness requirements predicted by the THOR equations for three different engines are tabulated in figure 7.

The thickness requirements predicted by the THOR equations are much larger than rings actually in service. Based on observation of published cross sections of engines in the

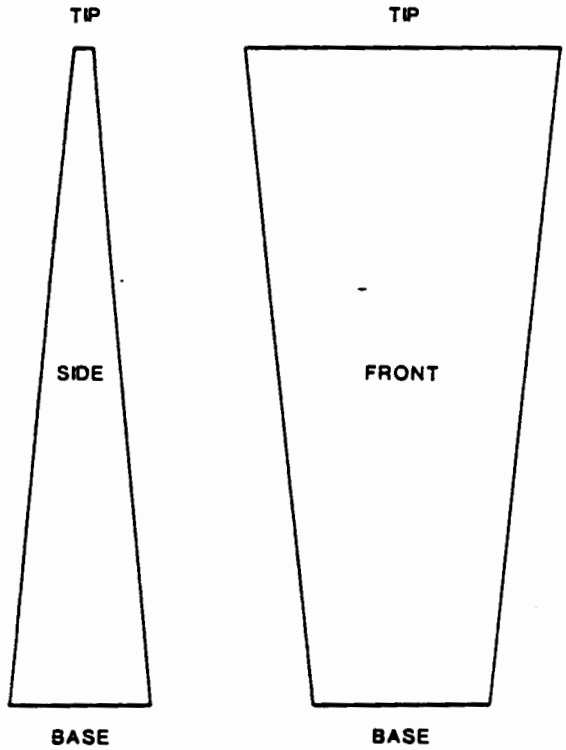


BASIC FAN BLADE GEOMETRY

NOTE: SEE FIGURE 4 FOR FAN BLADE DIMENSIONS.

THICKNESS OF BASELINE TITANIUM CONTAINMENT RINGS FOR TIP, BASE, AND SIDE IMPACTS BASED ON THOR EQUATIONS

| ENGINE MODEL | ENGINE THRUST (LB) | CONTAINMENT RING THICKNESS (IN.) | | |
|---|---|---|---|---|
| | | TIP IMPACT | BASE IMPACT | SIDE IMPACT |
| F109 | 1,330 | 3.172 | 2.158 | 0.854 |
| TFE731-5 | 4,500 | 4.455 | 3.019 | 0.983 |
| CFM56-2 | 24,000 | 10.900 | 7.398 | 1.864 |

FIGURE 7. TITANIUM CONTAINMENT RING THICKNESS BASED ON THOR EQUATIONS

thrust range of the CFM56-2, an actual titanium containment ring would be expected to fall in a thickness range between 0.25 and 0.75 inch. Use of the Snecma design equation given in Section 2.3 predicts the need for a 0.66 inch thick titanium containment ring for the CFM56-2. Both the observed and predicted values of thickness are much smaller than the THOR equation predictions shown in figure 7 for the CFM56-2. This led to the conclusion that the THOR equations cannot be used to directly predict containment ring thickness requirements.

This showed that results obtained from small armor test panels, with fragment simulating projectiles, do not scale up to actual fan blade hardware very accurately. Some possible reasons for this are that armor data are based on small flat panels and compact projectiles, while turbine engine data are based on ring-type structures and projectiles that simulate the dynamic behavior of actual fan blades. Unlike the compact fragment simulation projectiles used to generate armor data, fan blades buckle and break following contact with the containment ring so that their entire kinetic energy is not effective in producing a penetration. Further, the ring-type structure of an actual containment ring is more flexible than a typical armor panel, therefore the dynamic response of the system is substantially different.

### 2.5.2 Correlation of Armor and Actual Containment Design Information to Calculate $B_4C$/Spectra Thickness Requirements

Since it was not possible to accurately calculate containment ring thicknesses directly from armor test panel data, an approach that combined the results of spin pit containment testing with armor test panel data was adopted. The approach selected was to design the baseline Kevlar containment for a given thrust level using the results of the NASA/GE tests, described in Section 2.4., and to design the $B_4C$/Spectra to provide an equivalent degree of protection as the Kevlar.

Armor test panel data for Kevlar and $B_4C$/Spectra panels were compared (reference 8). The density of Kevlar versus that of $B_4C$/Spectra required to defeat the same threat was compared over the entire range of areal densities for which data were available. The results of this study were used to develop a relationship between the areal density/thickness of Kevlar and $B_4C$/Spectra required to defeat the same threat. This relationship, combined with the relationship of Kevlar thickness to blade kinetic energy discussed in Section 2.3, allowed the curves shown in figures 8 and 9 to be developed.

The resulting areal densities and thicknesses for Kevlar and $B_4C$/Spectra containment rings calculated using the above procedure are plotted in figures 10 and 11.

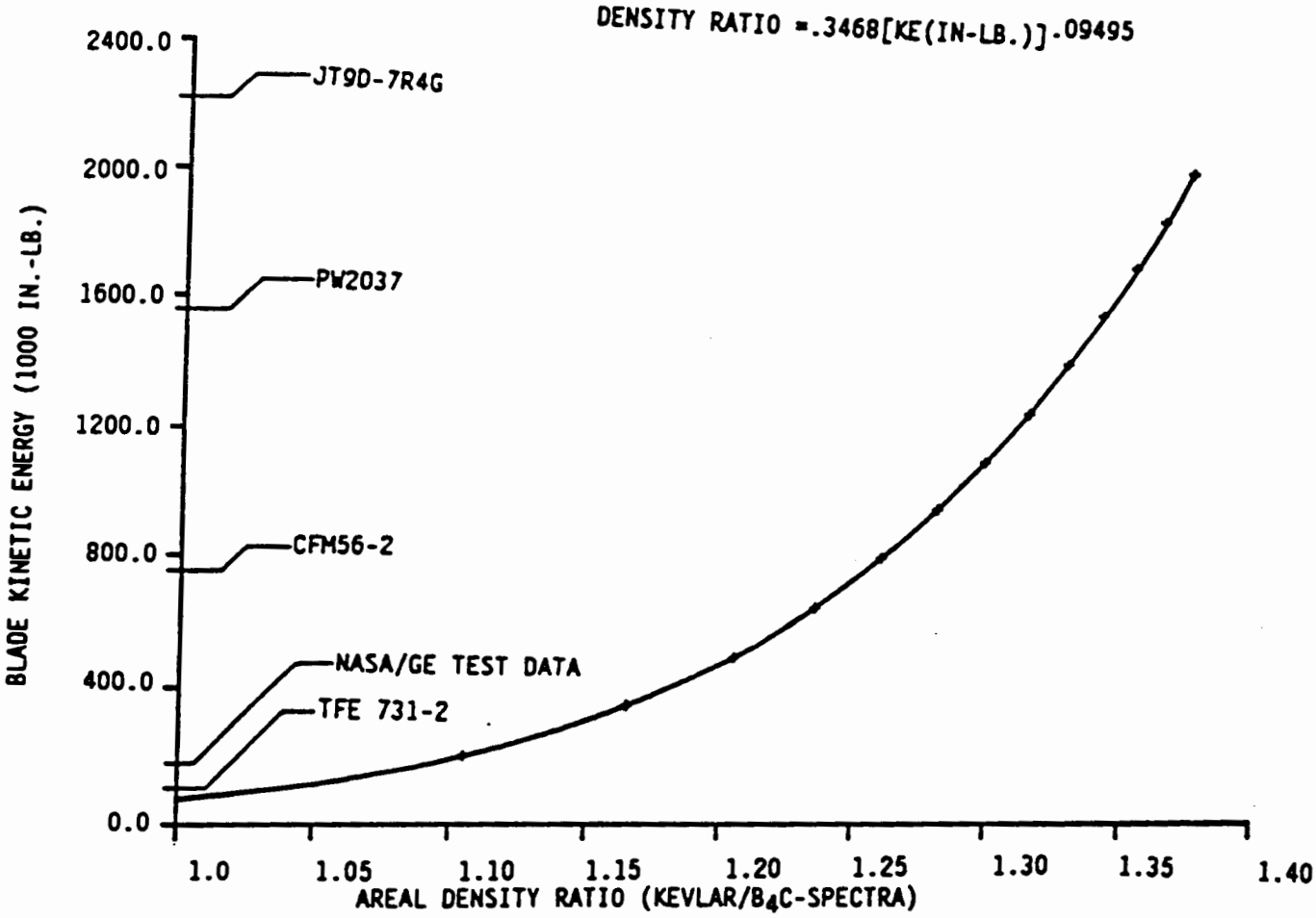


FIGURE 8. RATIO OF KEVLAR TO $B_4C$/SPECTRA AREAL DENSITY VERSUS FAN BLADE KINETIC ENERGY

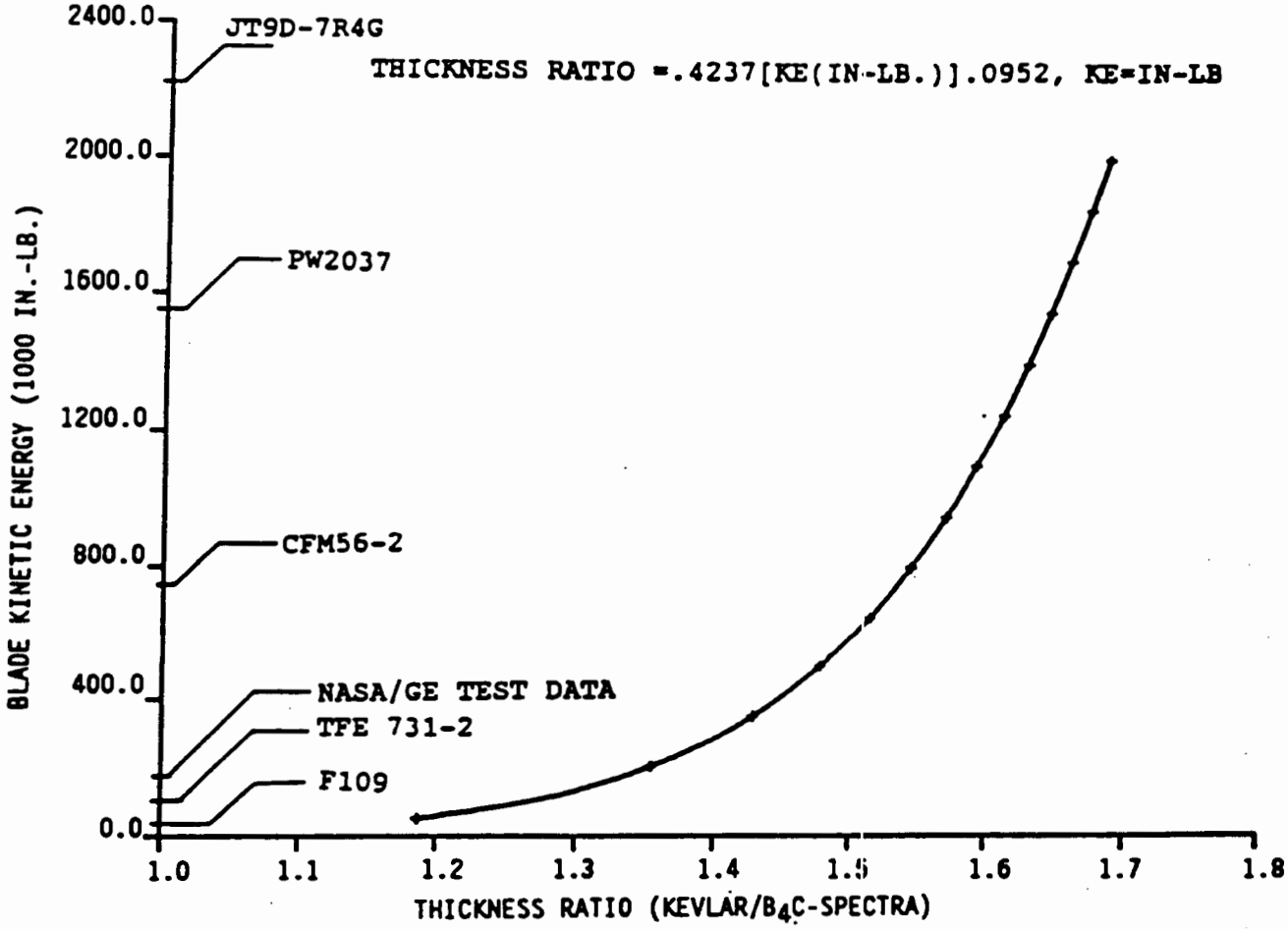


FIGURE 9. RATIO OF KEVLAR TO $B_4C$/SPECTRA THICKNESS VERSUS FAN BLADE KINETIC ENERGY

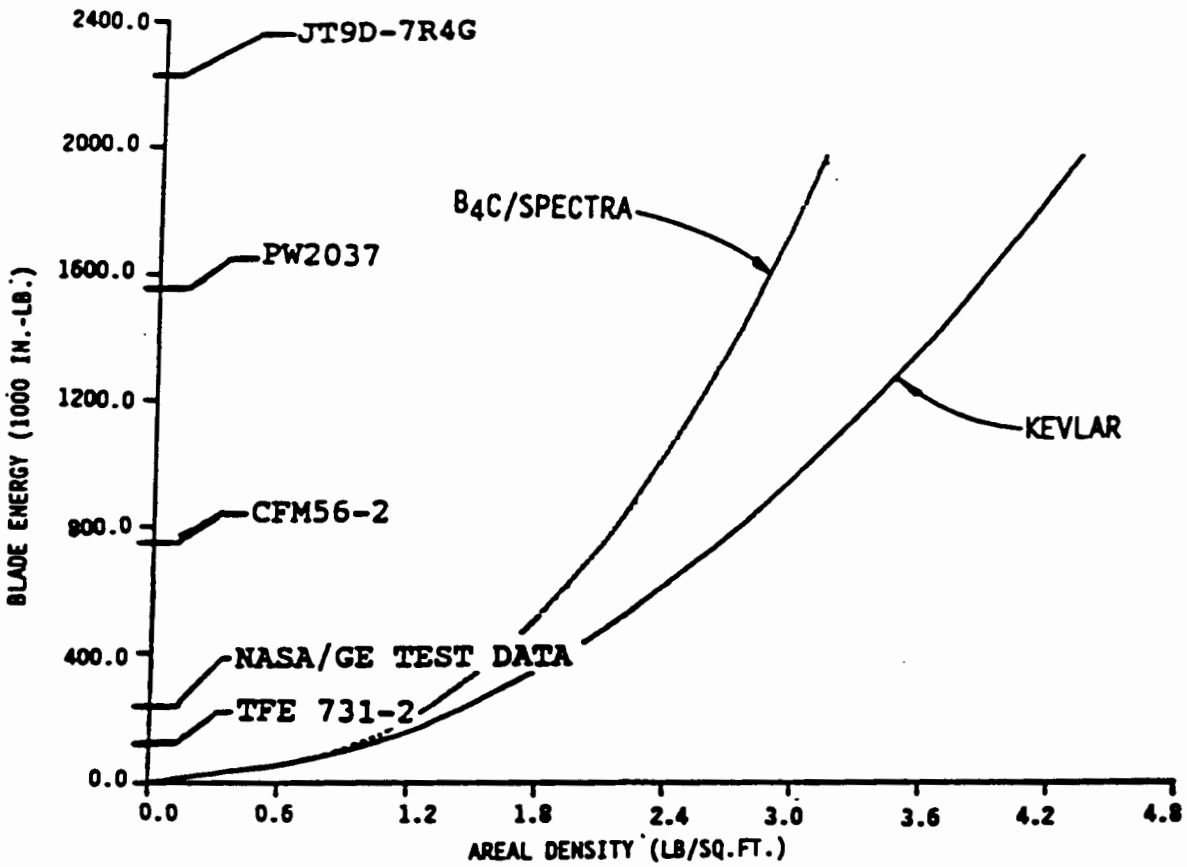


FIGURE 10. KEVLAR AND $B_4C$/SPECTRA CONTAINMENT RING AREAL DENSITY VERSUS BLADE KINETIC ENERGY

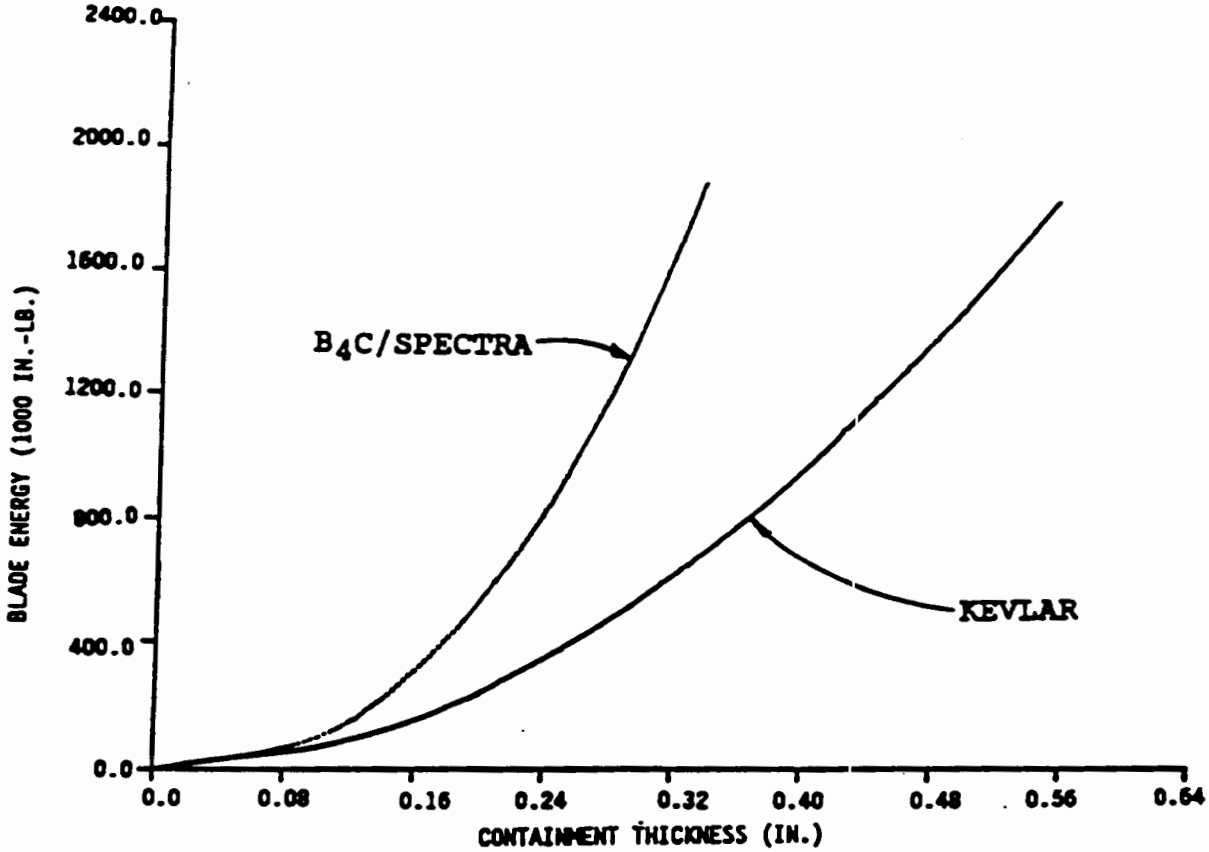


FIGURE 11. KEVLAR AND $B_4C$/SPECTRA CONTAINMENT RING THICKNESS VERSUS BLADE KINETIC ENERGY

## 3. CONCLUSIONS

3.1 Armor test data show that $B_4C$/Spectra is more weight effective than Kevlar for defeating projectile penetration.

3.2 The ratio of $B_4C$/Spectra weight effectiveness to that of Kevlar is larger for higher kinetic energy projectiles.

3.3 The weight effectiveness of $B_4C$/Spectra versus Kevlar containment is significant for engines of 20000 lb. or greater thrust.

## 4. REFERENCES


1. Payen,J.M., Containment of Turbine Engine Fan Blades, SNECMA, 6th International Symposium on Air Breathing Engines, Paris France, June 6-10, 1983, Symposium Papers A83-35801 16-07, AIAA, 1983, p. 611-616.

2. Heermann, K.F. and others, Study to Improve Turbine Engine Rotor Blade Containment, Aug. 1977, National Technical Information Service, Report No. FAA-RD-77-100.

3. Stotler, C., NASA-CR-165212, Development of Advanced Lightweight Containment Systems, May 1981.

4. Stotler, C. and Coppa, A.P., Containment of Composite Fan Blades, NASA CR-159544, July 1979.

5. Jane's All The World's Aircraft 1985-1986, Jane's Publishing Company Limited.

6. An Assessment of Technology for Turbojet Engine Rotor Failures, A Workshop held at MIT March 29-30, 1977, NASA CP-2017.

a. Types of Rotor Failure and Characteristics of Fragments, D. McCarthy, Rolls-Royce Limited Aero Division, Derby, United Kingdom.

b. Blade Fragment Energy Analysis, M.A.O'Connor, Jr., Douglas Aircraft Company, McDonnell Douglas Corporation.

c. Approaches to Rotor Fragment Protection, M.A.O'Connor, Jr., Douglas Aircraft Company, McDonnell Douglas Corporation.

d. Rotor Burst Protection Program: Experimentation To Provide Guidelines for the Design of Turbine Rotor Burst Fragment Containment Rings, G.J.Mangano, J.T.Salvino, R.A.DeLucia, Naval Air Propulsion Test Center, Princeton, NJ

e. Analysis of Simple 2-D and 3-D Metal Structures Subjected to Fragment Impact, D.A.Witmer, T.R.Stagliano, R.L.Spilker, J.J.A.Rodal, Aeroelastic and Structures Research Laboratory, Department of Aeronautics and Astronautics, Massachusetts, Institute of Technology.

f. Lightweight Engine Containment, A.T.Weaver, Pratt and Whitney Aircraft, United Technologies Corporation.

g. Numerical Analysis of Projectile Impact in Woven Textile Structures, David Roylance, Department of Materials Science and Engineering, Massachusetts Institute of Technology, Cambridge, Massachusetts.

h. Concepts for the Development of Light-Weight Composite Structures for Rotor Burst Containment, Arthur G. Holms, National Aeronautics and Space Administration, Lewis Research Center, Cleveland, Ohio.

i. Ceramic Composite Protection for Turbine Disc Bursts, P.B.Gardner, Industrial Ceramics Division, Norton Company.

j. Analysis methods for Kevlar Shield Response to Rotor Fragments, J.H.Gerstle, Boeing Commercial Airplane Company, Seattle, Washington.

k. Development of Fiber Shields for Engine Containment, R.J.Bristow, C.D.Davidson, The Boeing Company, Seattle, Washington.

l. Metallic Armor for Ballistic Protection from Steel Fragments, Donald F. Haskell, Ballistic Modeling Division, U.S. Army Ballistic Research Laboratory, Aberdeen Proving Ground, Maryland.

7. Holms, A.G., Concepts for the Development of Light-Weight Composite Structures for Rotor Burst Containment, NASA Lewis, 78N10084, March 1977.

8. Arndt, S.M. and Coltman, J.W., Summary of Armor Data Used to Evaluate Armor Systems for Application in the Containment of Turbine Fan Blades, TI-89422, Simula Inc., Phoenix, Arizona, April 7, 1989.

9. Project THOR Technical Report No. 47, The Resistance of Various Metallic Materials to Perforation by Steel Fragments; Empirical Relationship for Fragment Residual Velocity and Residual Weight, Army Materiel Command, Ballistics Research Laboratories, Aberdeen Proving Ground, Maryland, April, 1961.

## 5. BIBLIOGRAPHY


1. Hagg, A.C. and Sankey, G.O., The Containment of Disk Burst Fragments by Cylindrical Shells, Journal of Engineering for Power, Trans. ASME, Paper No. 73-WA-Pwr-2.

2. Sapowith, A.D., et. Al., State-of-the-art Review of Flywheel Burst Containment, Report No. UCRL-15257, May 1980.

3. Gunderson, C.O., Study to Improve Airframe Turbine Engine Rotor Blade Containment, Report No. FAA-RD-77-44, July 1977.

4. Lane, A., et al., A Design Review of Ceramic Components for Turbine Engines, Co-Author, ASME Report 79-GT-36.

5. Lane, A., et al., Material, Design and Test Aspects of Ceramic Component Development, Co-Author, ASME Report 81-GT-179.

6. Lane, A., et al., Ceramic Structural Design for the Garrett Model TSE331C-1, Metals and Ceramics Information Center, Report No. MCIC-78-36.

7. Lane, A., et al., Ceramic Combustor Design, Co-Author, Metals and Ceramics Information Center, Report No. MCIC-78-36

8. Coltman, J.W. and Arndt, S.M., Lightweight Aircrew Armor Design Program, Final Report, TR-86412, Simula Inc., Phoenix, Arizona: U.S. Army Aviation Applied Technology Directorate, Fort Eustis, Virginia, August 18, 1986.

9. Foltz, J.V., Fishman, S.G., Ballistic Penetration Studies on Advanced Lightweight Armor Materials, NSWC TR 80-53, Naval Surface Weapons Center, January 1980.

10. Rupert, N.L., Ballistic Characterization of Kevlar Composite Armor Systems Using Fragment Simulators, NSWC TR 79-92, Naval Surface Weapons Center, December 1978.

11. Abbott, K.H., Response of Lightweight Armor Materials to Impact by Simulated Fragments of Several Aspect Ratios, AMMRC TR 76-27, AMMRC Watertown, MA., September 1976.

12. Adams, D.F., Composite Materials in Armor Applications: Performance and Cost, RDA-TR-4400-002, Defense Advanced Research Projects Agency, July 1974.

13. Figucia, F., Energy Absorption of Kevlar Fabrics Under Ballistic Impact, ADA090390, U.S. Army Natick Research and Development Command, June 1980.

14. Salvino, James T., DeLucia, Robert A., Russo, Tracy, Experimental Guidelines for the Design of Turbine Rotor Fragment Containment Rings, Naval Air Propulsion Center, DOT/FAA/CT-88-21.

15. Marks' Standard Handbook for Mechanical Engineers, Eighth Edition, Baumeister,T., Avallone,E.A., Baumeister III,T., McGraw-Hill Book Co.

16. Salvino, J.T., Mangano, G.J., Delucia, R.A., Rotor Burst Protection: Design Guidelines for Containment, 79N27166 Issue 18, April 1979.

# APPENDIX A

## BASIC PROGRAM FOR CALCULATION OF BLADE KINETIC ENERGY

```
10 REMeTHIS PROGRAM CALCULATES FAN BLADE VOLUME AND CG AS A FUNCTION
20 REM OF HUB AND TIP RADIUS
30 REM
40 INPUT "ENGINE MODEL NUMBER";A$
50 INPUT "TIP DIAMETER";DT
60 RT =DT/2!
70 RH = .33*RT
80 INPUT "NUMBER OF BLADES";N
90 INPUT "BLADE DENSITY (LB/IN3)";RHO
100 INPUT "THRUST";THRUST
110 DIM R(40), T(40), C(40), V(40),RV(40)
120 RPM = 170168.4/RT
130 CT = (7.2257*RT)/N
140 CH = (17.2788*RH)/N
150 TT = .0275*CT
160 TH = .065*CH
170 FOR I = 1 TO 40
180 R(I) = RH + ((2*I-1)*(RT-RH)/80!)
190 C(I) = CT + (CH-CT)*((RT-R(I))/(RT-RH))
200 T(I) = TT + (TH-TT)*((RT-R(I))/(RT-RH))
210 V(I) =C(I)*T(I)*(RT-RH)/40
220 V =V +V(I)
230 RV(I) = R(I)*V(I)
240 RV = RV +RV(I)
250 R = RV/V
260 NEXT I
270 KE=.5*(((V*RHO)*(R^2!))/386.4)*(((RPM*2*3.1416)/60!)^2!)
280 WT = V*RHO
290 LPRINT "   "
300 LPRINT "  ***************************************************************"
310 LPRINT "   "
320 LPRINT "   ENGINE MODEL NO. - ";A$;"   THRUST =";THRUST;"   FAN SPEED =";RPM
330 LPRINT "   HUB DIAMETER ="; USING "##.###";2*RH
340 LPRINT "   TIP DIAMETER =";USING"##.###";DT
350 LPRINT "   NUMBER OF BLADES =";N
360 LPRINT "   BLADE WEIGHT = ";USING "##.####";WT
370 LPRINT "   RADIUS AT BLADE CG =";USING"##.###";R
380 LPRINT "   BLADE ROTATIONAL K.E. =";USING "##.###^^^^";KE
390 LPRINT "   "
400 LPRINT "   TIP THICKNESS =";USING".###";TT
410 LPRINT "   TIP CHORD LENGTH =";USING"##.###";CT
420 LPRINT "   HUB THICKNESS =";USING".###";TH
430 LPRINT "   HUB CHORD LENGTH =";USING"##.###";CH
440 LPRINT "   PERIMETER =";USING"##.###";2*(TT+TH)
450 LPRINT "   "
     780 END
```